

AD-A212 448

4

ORT DOCUMENTATION PAGE

1a. REPORT SECURITY CLASSIFICATION Unclassified			1b. RESTRICTIVE MARKINGS		
2a. SECURITY CLASSIFICATION AUTHORITY SEP 08 1989			3. DISTRIBUTION/AVAILABILITY OF REPORT Unclassified/Unlimited		
2b. DECLASSIFICATION/DOWNGRADING SCHEDULE			5. MONITORING ORGANIZATION REPORT NUMBER(S)		
4. PERFORMING ORGANIZATION REPORT NUMBER(S) ONR Technical Report 9			7a. NAME OF MONITORING ORGANIZATION Office of Naval Research		
6a. NAME OF PERFORMING ORGANIZATION Dept. of Chem. Eng. & Mat. Sci. Corrosion Research Center		6b. OFFICE SYMBOL (If applicable)	7b. ADDRESS (City, State, and ZIP Code) 800 North Quincy Street Arlington, VA 22217-5000		
6c. ADDRESS (City, State, and ZIP Code) University of Minnesota Minneapolis, MN 55455		9. PROCUREMENT INSTRUMENT IDENTIFICATION NUMBER Contract No. N00014-88-K-0360			
8a. NAME OF FUNDING/SPONSORING ORGANIZATION DARPA/ONR	8b. OFFICE SYMBOL (If applicable) Code 1113	10. SOURCE OF FUNDING NUMBERS			
8c. ADDRESS (City, State, and ZIP Code) 800 North Quincy Street Arlington, VA 22217-5000		PROGRAM ELEMENT NO.	PROJECT NO.	TASK NO.	WORK UNIT ACCESSION NO.
11. TITLE (Include Security Classification) Capacitive Behavior in Conducting Polymers		<div style="border: 1px solid black; padding: 5px;"> DISTRIBUTION STATEMENT 1 Approved for public release Distribution Unlimited </div>			
12. PERSONAL AUTHOR(S) Katsuhiko Naoi, Mary M. Lien, William H. Smyrl, and Boone B. Owens					
13a. TYPE OF REPORT Technical	13b. TIME COVERED FROM 7/88 TO 6/89	14. DATE OF REPORT (Year, Month, Day) 89/06/15		15. PAGE COUNT 19	
16. SUPPLEMENTARY NOTATION accepted for publication in Applied Physics Communication					
17. COSATI CODES		18. SUBJECT TERMS (Continue on reverse if necessary and identify by block number)			
FIELD	GROUP	SUB-GROUP			
		conducting polymer; capacitance; polypyrrole; lithium cell			
19. ABSTRACT (Continue on reverse if necessary and identify by block number)					
<p>The over-all differential capacitance for conducting polymers like polypyrrole and polyvinylferrocene which show a very high redox capacity for the oxidation/reduction process was modeled as a function of applied voltage from the cyclic voltammetric data. The capacitance values are compared with various types of carbon double layer and conventional capacitor devices. Also, the theoretical capacitance values for a cell was estimated by assuming a hypothetical minimum equivalent cell consisting of an anode (Li), a cathode (polypyrrole) and an electrolyte solution ($2 \text{ mol dm}^{-3} \text{ LiClO}_4(\text{PC})$) without any hardware. The charge/discharge process or doping/undoping process was determined by impedance analysis and the limiting capacitance was estimated. Also, an attempt was made to separate the faradaic and capacitive currents according to the theory of the impedance of diffusion in a layer of finite thickness.</p> <p style="text-align: center; font-size: 2em;">89 9 7 038</p>					
20. DISTRIBUTION/AVAILABILITY OF ABSTRACT <input checked="" type="checkbox"/> UNCLASSIFIED/UNLIMITED <input type="checkbox"/> SAME AS RPT <input type="checkbox"/> DTIC USERS			21. ABSTRACT SECURITY CLASSIFICATION Unclassified		
22a. NAME OF RESPONSIBLE INDIVIDUAL Boone B. Owens			22b. TELEPHONE (Include Area Code) (612) 625-1332	22c. OFFICE SYMBOL	

CAPACITIVE BEHAVIOR IN CONDUCTING POLYMERS

Katsuhiko Naoi, Mary M. Lien, William H. Smyrl and Boone B. Owens

Corrosion Research Center
Department of Chemical Engineering & Materials Science
University of Minnesota
221 Church St. SE, Minneapolis MN 55455, U.S.A.

ABSTRACT

The over-all differential capacitance for conducting polymers like polypyrrole and polyvinylferrocene which show a very high redox capacity for the oxidation/reduction process was modeled as a function of applied voltage from the cyclic voltammetric data. The capacitance values are compared with various types of carbon double layer and conventional capacitor devices. Also, the theoretical capacitance values for a cell was estimated by assuming a hypothetical minimum equivalent cell consisting of an anode(Li), a cathode(polypyrrole) and a electrolyte solution ($2 \text{ mol dm}^{-3} \text{ LiClO}_4(\text{PC})$) without any hardware. The charge/discharge process or doping/undoping process was determined by impedance analysis and the limiting capacitance was estimated. Also, an attempt was made to separate the faradaic and capacitive currents according to the theory of the impedance of diffusion in a layer of finite thickness.

INTRODUCTION

Conducting polymers including electrically-conducting polymers and redox polymers have a wide range of applications in the field of electronic devices because they show high electroactivity and concurrent reversible doping/undoping of ions from aqueous and non-aqueous solutions(1-9). Especially, in non-aqueous solutions with poor nucleophilic character, these

Approved For	
WHS CRASH	<input checked="" type="checkbox"/>
DTIC TAB	<input type="checkbox"/>
Unannounced	<input type="checkbox"/>
Justification	
By	
Distribution	
Availability Codes	
Dist	Availability Codes
A-1	



polymers show a fairly high electroactivity(8,9). Due to this advantage, one of the most promising applications is the utilization of the electrode material as the cathode, the anode or both in energy storage devices such as capacitors(1-3) or rechargeable batteries(8,9). In this paper, the authors describe the large capacitive effect observed in conducting polymers, especially, polypyrrole(PPy). Using three different methods, *i.e.*, cyclic voltammetry, impedance and quartz crystal microbalance(QCM) measurements, the variations in capacitance and doping of anions for PPy and PVF films are compared to the mass changes that occur during the charge-discharge process. Two different categories of polymers were chosen on the basis of previous results(5, 7-9). The first is the redox polymer, PVF which was spin-coated on a gold-coated silicon wafer substrate. In PVF active sites are located in the ferrocene group pendant to the vinyl chain shown in Fig.1. The oxidation-reduction accommodates up to 100% anion doping. The second polymer is PPy which was polymerized electrochemically to a similar substrate. PPy is a heterocyclic polymer which exhibits a doping level up to about 35%, and the active sites are delocalized in 3 monomer units(see Fig.1). Each polymer has distinctive features in structure and electrochemical response, but the main difference is the relative balance of the faradaic process and the capacitive charging process.

EXPERIMENTAL

Preparation of Polymer Films

PPy films were deposited by oxidative electropolymerization at 0.8 V vs. Ag/Ag⁺(0.01 M AgNO₃) on Au which was evaporated on silicon wafers(5,7). PVF (MW=80,000) films were spin-coated from a methylene chloride solution on silicon wafers which had been coated with 1000Å gold by evaporation. The entire disk was flooded with PVF solution and the disk was rotated at 200-300 rpm for 10 seconds. The thicker films were prepared by increasing the initial concentration of PVF and/or applying one more coat. The 3" wafers were cut into smaller pieces and a wire was attached to the gold substrate. Spin-coated PVF films are very stable following the initial break-in cycle, showing no deterioration after 2-3 days immersion in the electrolyte. For the QCM

measurements the sample preparation was identical, except that the substrate for each film was a gold coated quartz crystal.

Quartz Crystal Microbalance Measurements

Shear mode 6MHz AT-cut quartz crystals(INFICON) were used for this investigation(7). The crystals had vacuum deposited gold electrodes on both sides. With a total projected area exposed to the solution($0.1 \text{ mol dm}^{-3} \text{ LiClO}_4$ in acetonitrile) of 0.33 cm^2 , the quartz plate was sealed to the cell with a silicone rubber sealant. The resonance frequency shift, which has a linear relationship with the mass change(10) was measured with a frequency counter, and the data was stored in a personal computer. Experiments were carried out under nitrogen. The conducting polymer film in contact with the solution was the working electrode which was grounded through the potentiostat. The oscillator was isolated from the potentiostat with a $1 \mu\text{F}$ capacitor in order to avoid dc polarization of the crystal.

Impedance Measurements

An ac voltage signal(maximum amplitude = 5 mV peak to peak) superimposed on a dc bias was applied to the cell as a perturbation, and the response current signal was analyzed using FFT techniques(4-6). The range of frequencies was 5 mHz to 100 kHz.

PDIM Measurements

The Phase Detection Microscope(ZYGO MAXIM 3D Laser Interferometric Microscope) measures vertical heights over a moderately large surface area using the technique of optical phase-measurement interferometry. This technique is similar to but considerably more accurate, rapid, and more powerful than traditional visual detection of the curvature of interference fringes resulting from light reflected from a texture surface. The vertical resolution of the microscope is limited primarily by stray vibrations and is specified by the manufacturer to be 0.6 nm(11).

RESULTS AND DISCUSSION

Figure 1 is a typical comparison of the cyclic voltammograms for PPy

and PVF. PVF shows one set of sharp redox peaks, indicative of 100% redox behavior, and shows nearly Nernstian behavior. On the other hand, PPy shows a plateau region subsequent to a broad redox peak, which causes a large capacitive effect. Characterization of the processes which cause such behavior in the cyclic voltammogram and impedance is still unclarified because of the superposition of capacitive currents on the redox process. The large capacitive effect in some conducting polymers has been explained in several ways. For example, double-layer formation(3), over-doping of anions(1,2), and non-Nernstian redox processes(2) have been proposed as possible explanations. This analysis is continuing in our laboratory.

Super Capacitive Behavior in Conducting Polymers & Estimation of Differential Capacitance

In order to calculate the redox capacity for polymer electrodes, the typical cyclic voltammogram was used where the volume and the weight of polymer were well defined. Two steps were used to evaluate the differential capacitance of the polymer material(see Fig.2). First, the current under the cyclic voltammogram was integrated with respect to time to get the coulombic charge, $Q(\mu\text{C})$, as a function of voltage. Second, the charge-voltage curves were transformed to capacitance, $C(\text{F/cc})$, vs. potential profiles by differentiating with respect to potential. The capacitance value is expressed in units of Farads per cubic centimeter of polymer electrode material.

Figure 3 shows the charge-voltage curve and differential capacitance curve for a typical spin-coated PVF. There is a rapid increase of charge up to a point slightly anodic of $E_{1/2}$, but, no accumulation of charge is observed beyond this potential. The maximum differential capacitance amounts to over 2000 F/cc during the charging process, and during discharge, the value is slightly smaller than 2000 F/cc, probably within the uncertainty of the data analysis.

In contrast, PPy shows quite different behavior. There are two distinct regions in the charge-voltage curve. First, there is a rapid increase of charge below $E_{1/2}$, but charge continues to accumulate after the redox peaks. The first region is associated with the redox process, and the latter region is due to the capacitive current observed following the redox peak. The maximum capacitance is over 2000 F/cc for oxidation and 1400 F/cc for reduction. The

shape is not quite symmetrical in this case, but it sustains about 400 to 500 F/cc in the plateau region which covers a wide potential range.

In Fig.4a), the capacitance per unit weight of polypyrrole(Farads per gram, assuming $d=1.48$ g/cc) is compared to that of three different types of high surface area carbons, graphite powder, carbon black, and active carbon and the BET surface areas are 10, 20-275, 140-190 m^2/g , respectively. Their respective capacitance values are 2 to 4, 20 to 275 and 40 to 190 F/g. PPy shows a higher value than any of these carbon materials, because it exhibits the redox process in addition to the capacitive charging process characteristic of the carbons.

A further comparison can be made on the basis of an electrochemical cell with one of the polymers as an electrode. The comparison will be made to capacitor devices based on dielectric oxides or double layer charging that have been commercially available. The capacitance value per unit volume(1cc) was first calculated for a hypothetical equivalent cell(V_{cell}). The minimum equivalent volume for an anode(V_{Li}) and electrolyte($V_{Electrolyte}$) in $Li/2M LiClO_4(PC)/PPy$ is expressed as a function of cathode volume(V_{PPy}) and the capacitance value per cell is reduced by a factor of 4.85 to that per PPy according to the following calculation:

$$V_{cell} = V_{PPy} + V_{Li} + V_{Electrolyte} \quad [1]$$

$$V_{cell} = V_{PPy} + \frac{d_c V_{PPy} y_{max}}{M_c} \frac{M_a}{100 d_a} + \frac{d_c V_{PPy} y_{max}}{M_c} \frac{1000}{100 \cdot 2} \quad [2]$$

where d_c , M_c , d_a , M_a , y_{max} represent the density(1.48 g/cc) and monomer molecular weight(65 g/mol) of the PPy cathode, the density(0.53 g/cc) and molecular weight(6.94 g/mol) of the Li anode, and the maximum doping level of 40% for PPy.

$$V_{cell} = 4.85 V_{PPy} \quad [3]$$

For a 1cc $Li/2M LiClO_4(PC)/PPy$ cell, the maximum capacitance value amounts to 340 F/cc on oxidative-charging and 240 F/cc during discharge. The average capacitance values for both processes are about 120 F/cc. The applied

potential range for the calculation was from 2.0 to ca. 3.5 V vs. a Li electrode. The average capacitance is compared with those of existing capacitor devices as shown in Fig.4b). The capacitors compared are Al, Ta, Ceramic and also the electrochemical double layer cells (silver/carbon cell with solid electrolyte of RbAg_4I_5). Even though the value for the Li/PPy cell is a hypothetical value, the value is more than one order of magnitude higher than the best conventional systems. It is concluded that a Li/PPy has a potential for utilization as a high capacitor device.

QCM Analysis : Mass Change during The Charge/Discharge Process for PVF and PPy Electrodes

To analyze the doping/undoping process for PPy and PVF films, the in-situ mass change occurring during cyclic voltammetry was monitored using the electrochemical QCM method(10,11). Figure 5 shows typical QCM data obtained for the PVF and PPy electrodes. The mass change was monitored during cyclic voltammetry at 1 mV/s. The mass change curve for the PVF films was fairly reproducible and no hysteresis was observed. In contrast, polypyrrole shows some hysteresis for the variation of mass change, so the curves for oxidation and reduction scans do not agree. The hysteresis is due to different intrinsic rates for the charging and the discharging processes, and this is reflected in the cyclic voltammograms as well. The mass changes indicate that the doping and undoping processes are more complicated than might be evaluated from the electrochemical behavior above.

Impedance Analysis : Potential Variation of Low Frequency Faradaic and Capacitive Current for PPy Electrodes

In order to further analyze the doping and undoping behavior of PPy film, the impedance technique was used. Figure 6 shows a typical Cole-Cole plot for a polypyrrole films compared with a PVF film. Both films show a limiting diffusion process or finite thickness effect(4,5). For the PVF film, a typical planar electrode behavior is shown, but the PPy film shows a typical rough electrode behavior(5). In the latter case, the magnitude of the impedance is related to the square root of the impedance for a planar electrode, and the phase angle declines to half that of a planar electrode. There are three different

regions in the Cole-Cole plot. In the high frequency region, the electrode process obeys the Butler-Volmer equation, and is charge transfer-controlled. In the intermediate frequency region, the over-all electrode process is diffusion controlled. From the lowest frequency region where charge saturation is observed, one can estimate the limiting capacitance, C_L , using the relationship derived elsewhere(4,5). Values of C_L were estimated from the low frequency impedance data (charge saturation region: $\omega < \frac{L^2}{D}$). In this frequency range, the phase angle approached $\frac{\pi}{2}$ and C_L was calculated using the following equation[4].

$$\frac{1}{C_L} = \frac{d(-Z_i)}{d(\omega^{-1})} \quad [4]$$

where Z_i , C_L , D , and L are the imaginary component of impedance, the low frequency redox capacitance, diffusion coefficient, and the polymer film thickness respectively.

Figure 7 shows the capacitance of a PPy film estimated by cyclic voltammetry and impedance. The capacitive element estimated from the impedance measurement is smaller than the capacitance from cyclic voltammetry. This is due to the fact that the C_L is only associated with the faradaic process.

Finally, the PPy mass changes estimated from the three methods, i.e., cyclic voltammetry, QCM and impedance, are compared in Fig.8. The mass from the impedance measurement is the smallest because it only reflects the faradaic trapping. The value from the QCM data is slightly higher than that from impedance. This is due to the so-called the boundary effect on QCM measurements that arises because the surface film is flexible, and it has a different relaxation time compared to that of a rigid surface. The QCM can not detect the true weight gain in such a circumstance, and the rough, open structure of the PPy films used here(8,9), apparently caused the deviation. On the other hand, the mass changes are much higher than those observed with the QCM measurements.

For PVF films, there is good agreement of the capacitance values estimated from impedance and cyclic voltammetry measurements (5a). In the

case of PVF films, the behavior is completely different from that of PPy films.

These facts are related to the doping process of the two films. Figure 9 shows the Phase Detection Interferometric Microscope (PDIM) profile, and a brief schematic of the doping model for PVF and polypyrrole films. For PVF films, the doping process is fairly straightforward. The trapping of anions is mostly associated with the faradaic process, and shows very little surface charging because the film is flat and compact. In the PDIM profile, the average peak-to-valley height of the PVF film is only 38.9nm, so the surface is very smooth. For such a compact film, it is very likely that a volumetric increase due to solvent uptake is seen at the high doping level of anion insertion into the polymer phase. On the other hand, for the polypyrrole film, the doping process is much more complicated. There seem to be two kinds of trapping when the active sites are neutralized with the negative charge of anions. The first is deep trapping and the second is a weak or surface trapping. The deep trapping is associated with the faradaic current, and the weak trapping corresponds to the large capacitive charging because the effective surface area is very large. The shallow trapping of the surface cannot be detected by QCM measurements, because the polymer chain is not rigid. Also, it is likely that the displacement of solvent occurs by insertion of a large anion into the interior of the polypyrrole polymer layer, and this should be more important in polypyrrole ($d=1.48$) which is more dense than PVF ($d=0.42$).

We conclude that both redox and conducting polymers show large specific capacitances that may be useful in high energy capacitor devices. Although the mechanism responsible for the large capacitance densities is suggested above, more work is needed for complete characterization.

ACKNOWLEDGEMENT

The authors wish to acknowledge the financial support of the Defense Advanced Research Projects Agency and the Office of Naval Research.

REFERENCES

- 1) S. W. Feldberg, *J. Am. Chem. Soc.*, **106**, 4671 (1984).
- 2) B. J. Feldman, P. Burgermayer and R. W. Murray, *ibid.*, **107**, 872

- (1985).
- 3) (a) J. Tanguy, N. Mermiloid and M. Hoclet, *Synth. Met.*, **18**, 7 (1987).
(b) J. Tanguy and N. Mermiloid, *ibid.*, **21**, 129 (1987).
(b) J. Tanguy, N. Mermiloid and M. Hoclet, *J. Electrochem. Soc.*, **134**, 795 (1987).
 - 4) C. Ho, I. D. Raistrick and R. A. Huggins, *ibid.*, **127**, 343 (1980).
 - 5) (a) T. B. Hunter, P. S. Tyler, W. H. Smyrl and H. S. White, *ibid.*, **134**, 2198 (1987);
(b) K. Naoi, K. Ueyama, T. Osaka and W. H. Smyrl, *ibid.*, submitted for publication.
 - 6) T. Osaka and K. Naoi, *Bull. Chem. Soc. Jpn.*, **55**, 36 (1982).
 - 7) M. Lien and W. H. Smyrl, Proc. of 174th ECS Meeting(Trans. Tech. in Corr. Sci & Eng.), p.286 (1988).
 - 8) T. Osaka, S. Ogano, K. Naoi, and N. Oyama, *J. Electrochem. Soc.*, **136**, 306 (1989).
 - 9) (a) K. Naoi and T. Osaka, *J. Electrochem. Soc.*, **134**, 2479 (1988);
(b) K. Naoi, B. B. Owens, M. Meda and T. Osaka, Proc. of 174th ECS Meeting, Chicago (1988), **88-6**, 770 (1988).
(c) K. Naoi, K. Ueyama and T. Osaka. *J. Electrochem. Soc.*, in press.
 - 10) (a) P. T. Varineau and D. A. Buttry, *J. Phys. Chem.*, **85**, 389 (1987);
(b) M. D. Ward, *ibid.*, **92**, 2049 (1987);
(c) M. D. Ward, *J. Electrochem. Soc.*, **135**, 2747 (1987).
 - 11) W. H. Smyrl, R. T. Atanasoski, L. Atanasoski, L. Hartshorn, M. Lien, K. Nygren and E. A. Fletcher, *J. Electroanal. Chem.*, **264**, 301 (1989).

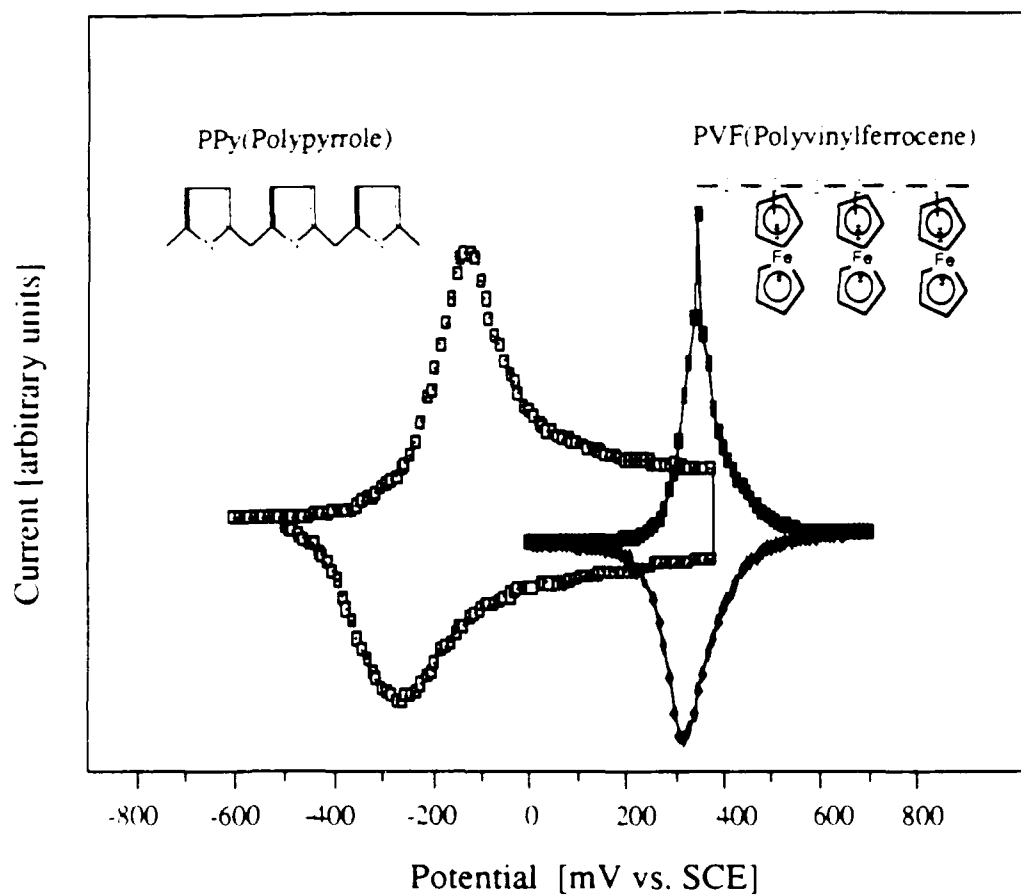


FIGURE 1 Cyclic voltammograms for polyvinylferrocene(PVF) and polypyrrole(PPy) films in $0.1 \text{ mol dm}^{-3} \text{ LiClO}_4/\text{acetonitrile(AN)}$ at a scan rate of 0.1 mV s^{-1} .

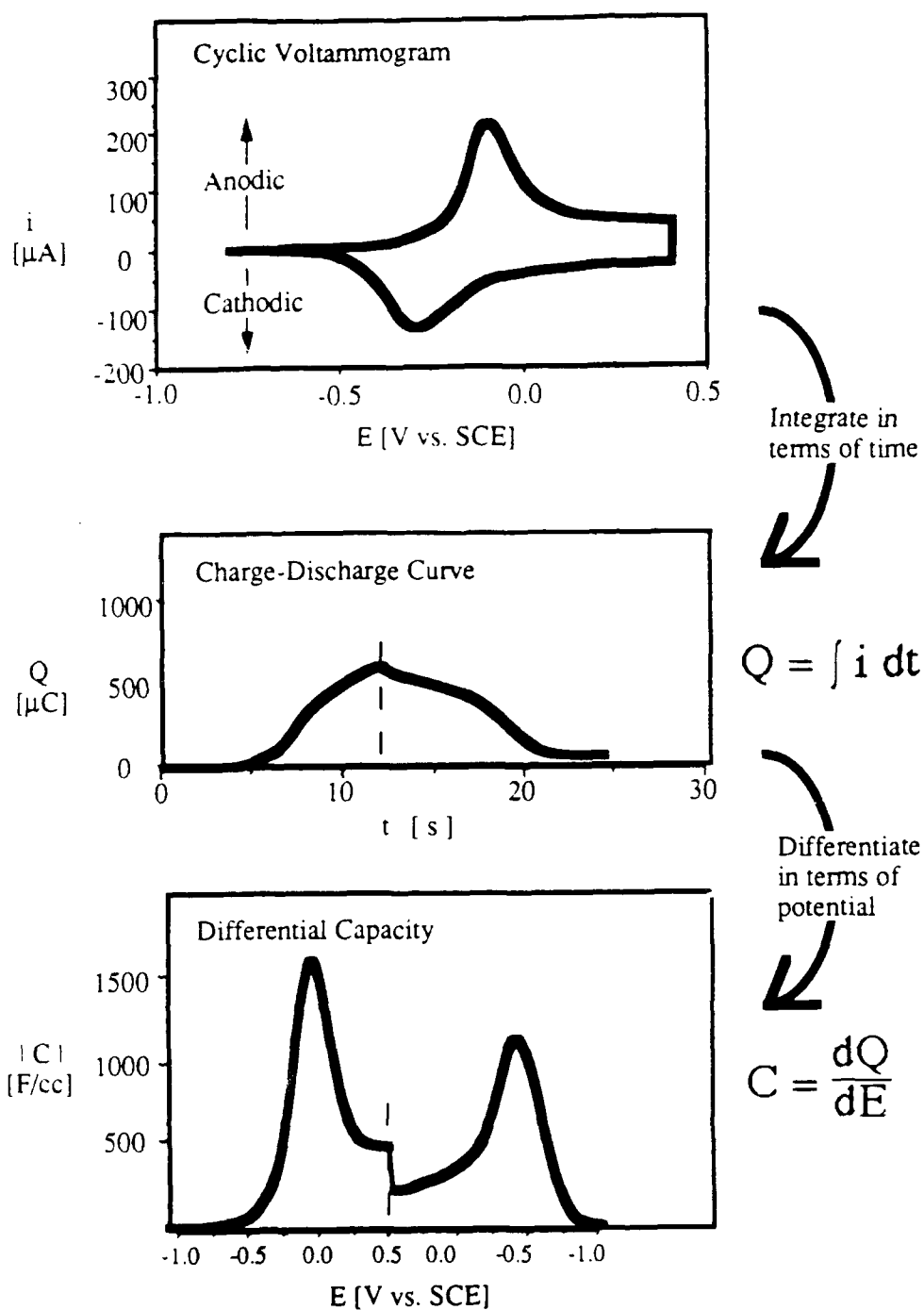


FIGURE 2 Calculation procedure of charge-voltage characteristics and differential capacitance.

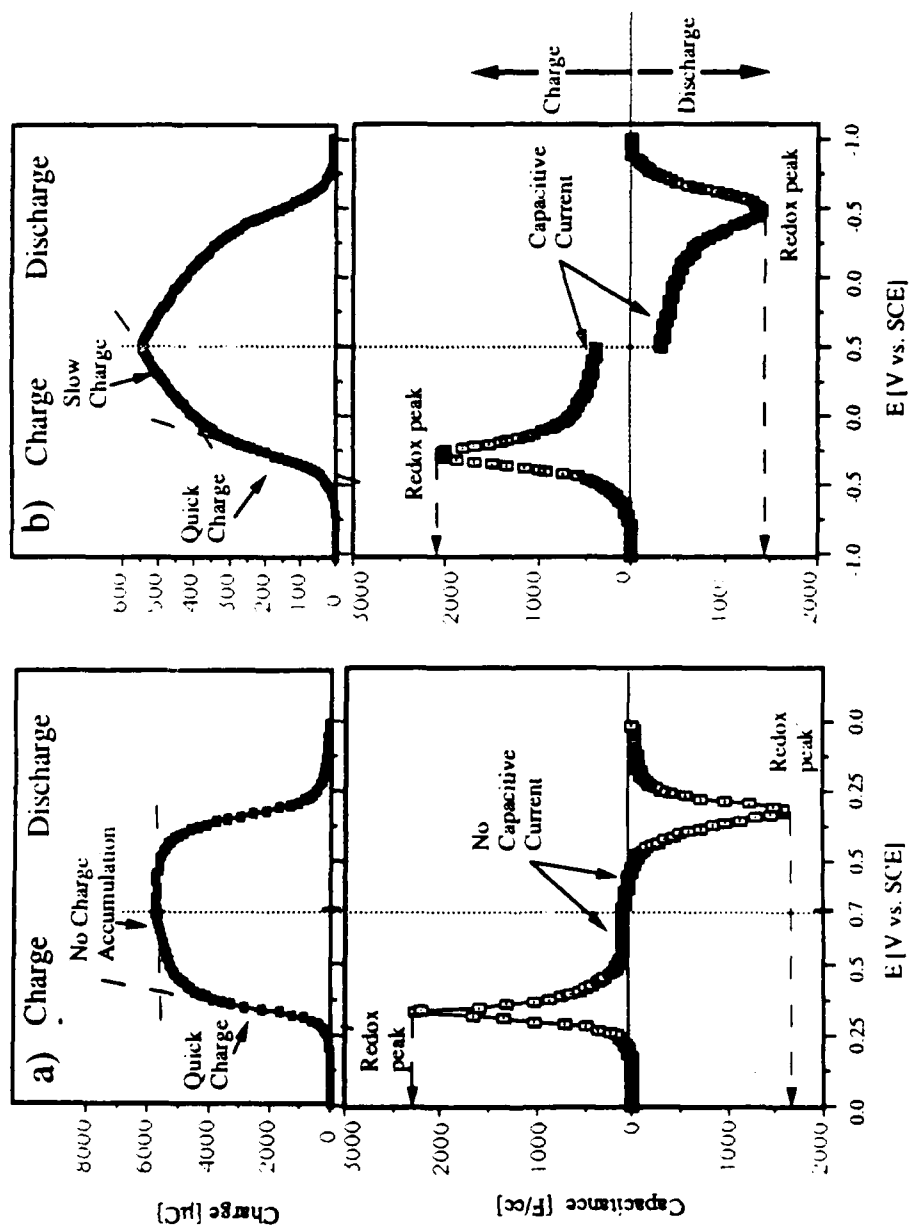


FIGURE 3 Charge-voltage characteristics and differential capacitance variations for (a)PVF and (b)PPy films.

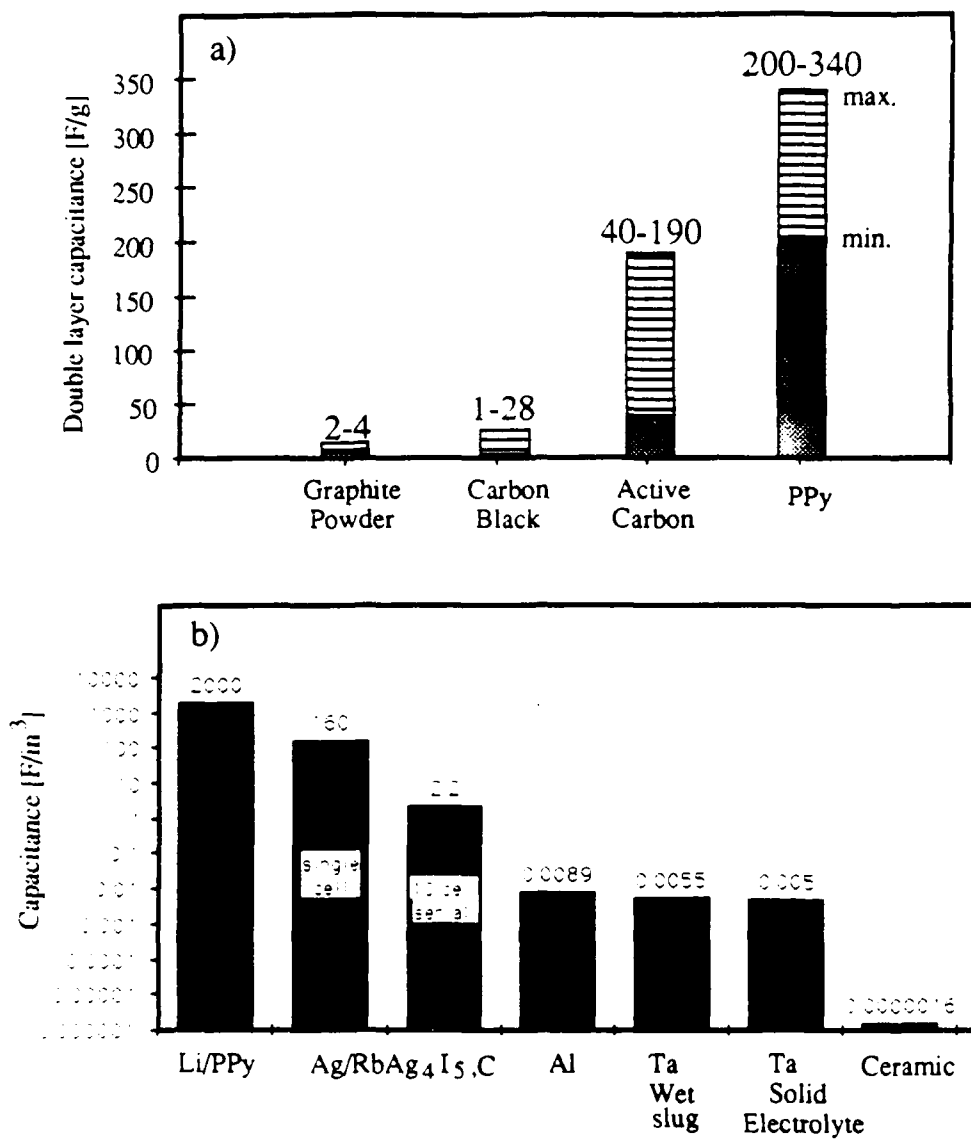


FIGURE 4 Comparison of capacitance values of PPy or Li/PPy cells to carbon as a single electrode(a) and as a cell(b).

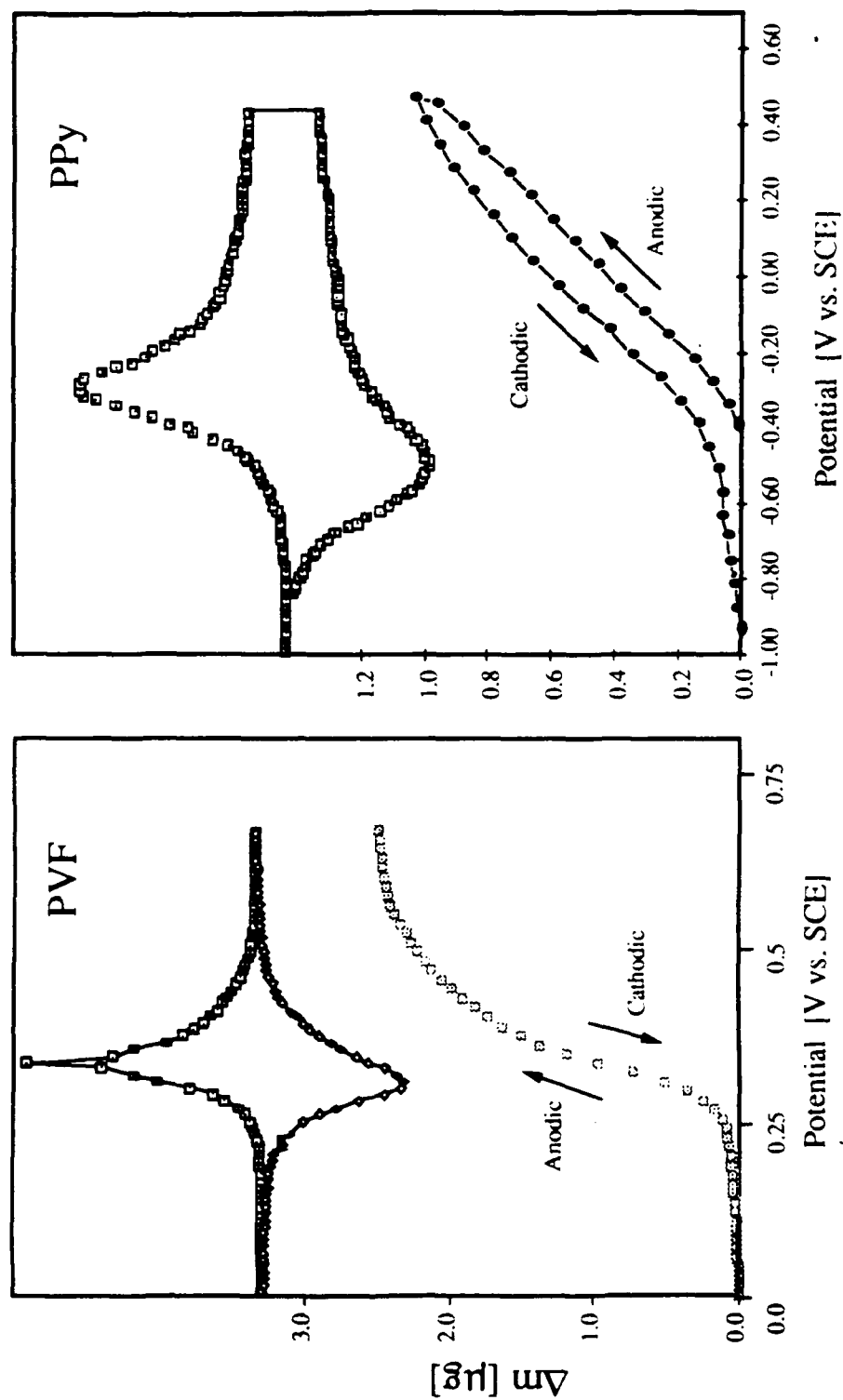


FIGURE 5 Typical mass change at PVF and PPy electrodes during cyclic voltammetry at 1 mV s^{-1} are compared to the respective cyclic voltammograms from Fig.1.

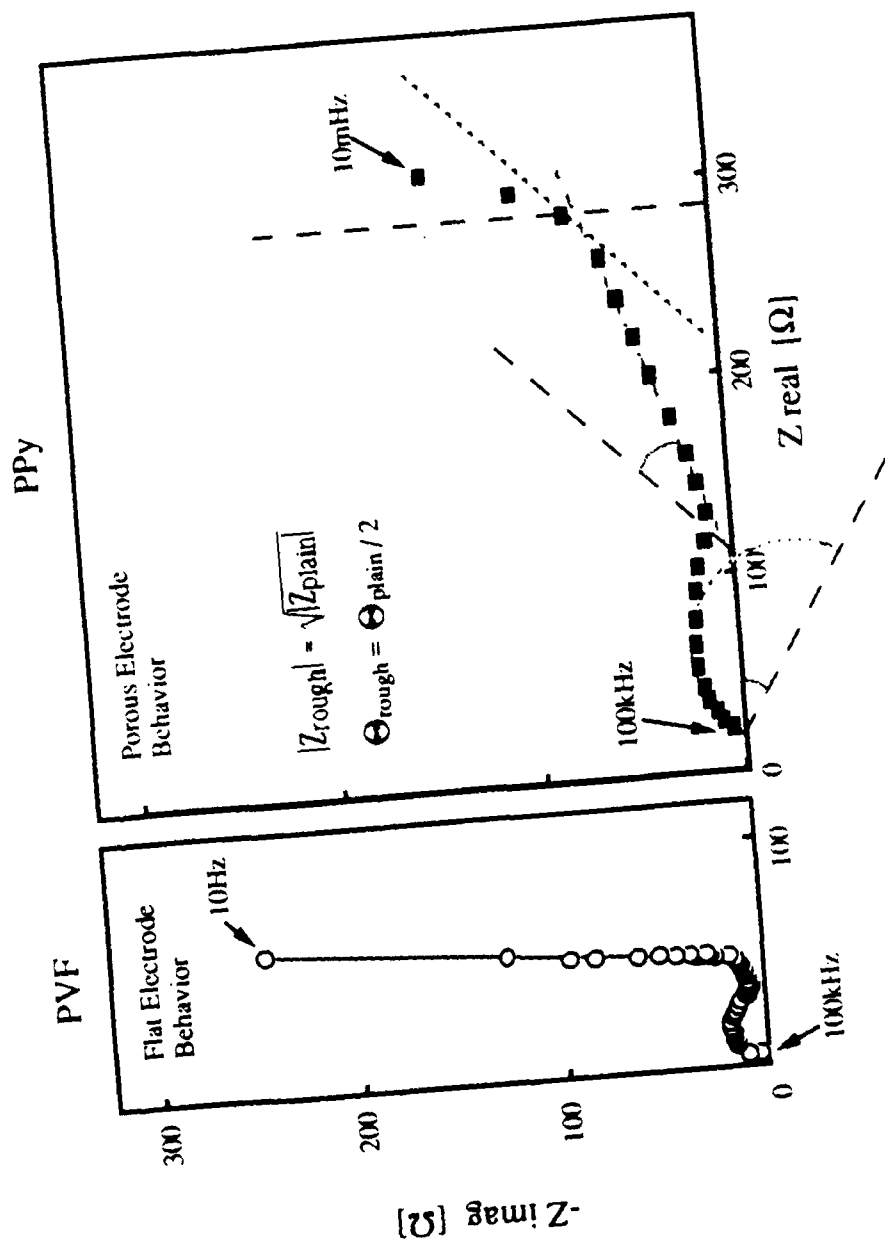


FIGURE 6 Typical Cole-Cole plots for PVF and PPy electrodes. Frequencies are indicated in the figure.

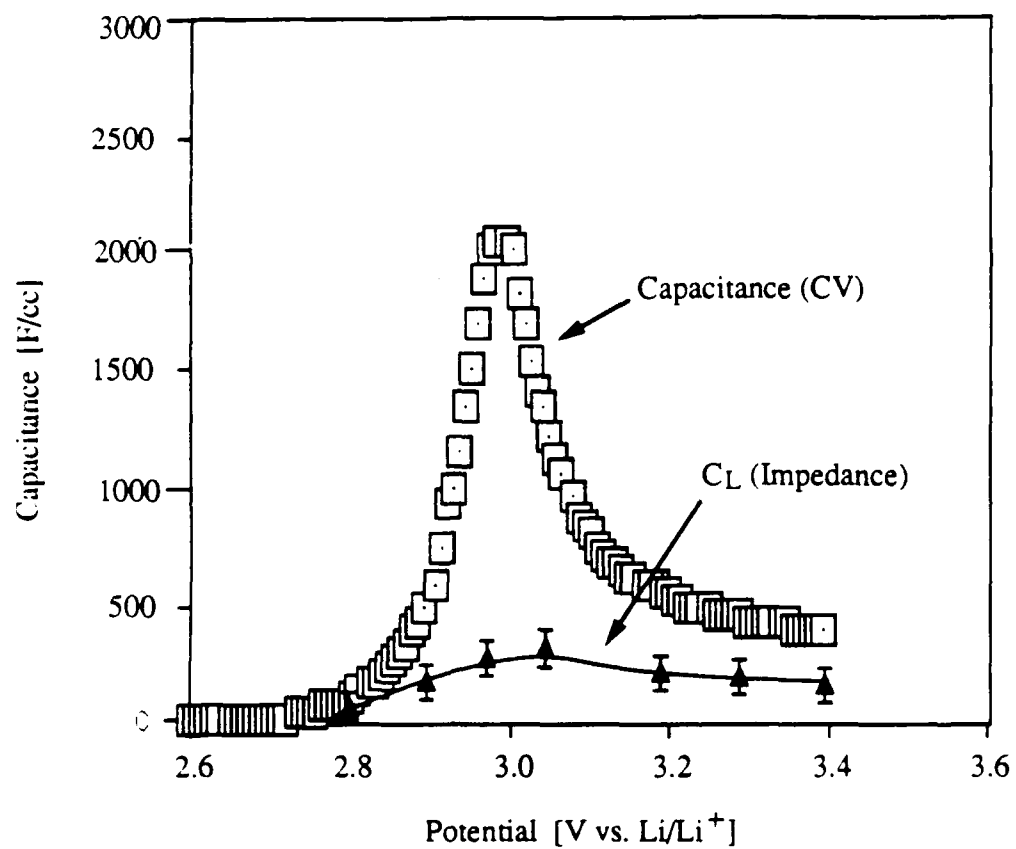


FIGURE 7 Variation of capacitance values (derived from low frequency values) against potential for PVF and PPy electrodes.

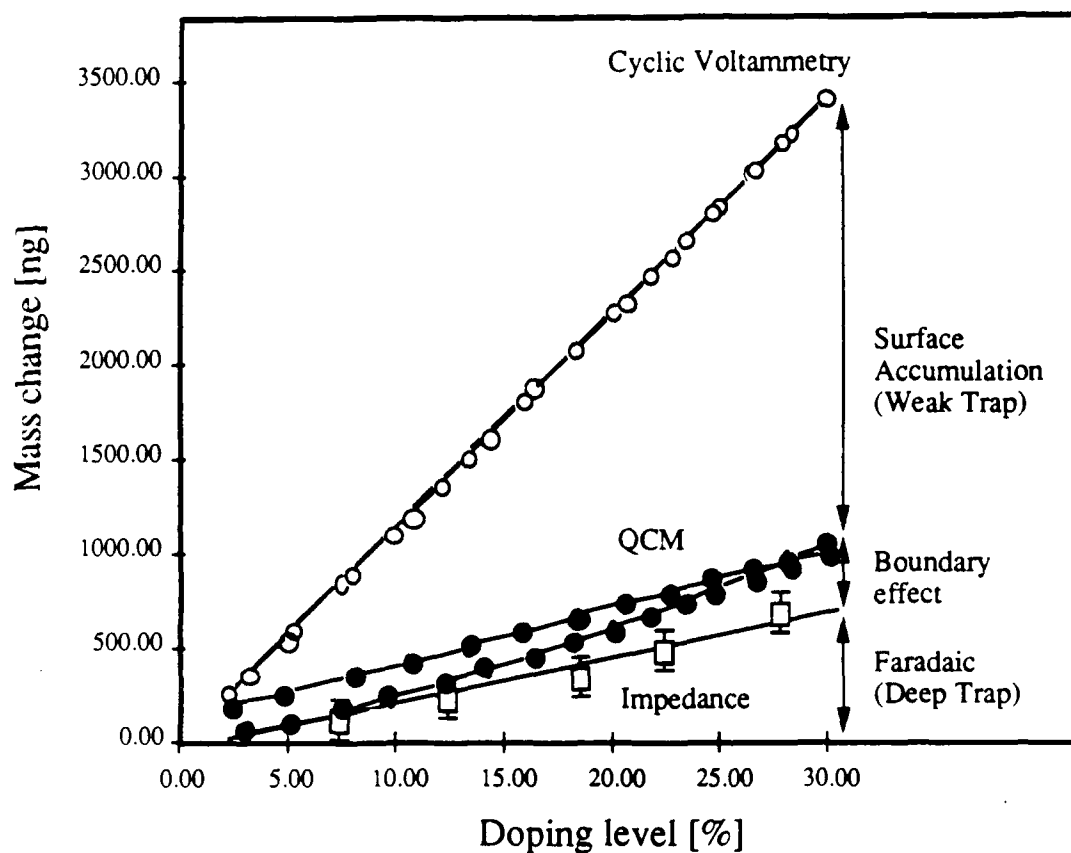


FIGURE 8 Comparison of the mass change at PPy electrodes with three different methods: cyclic voltammogram, QCM and impedance.

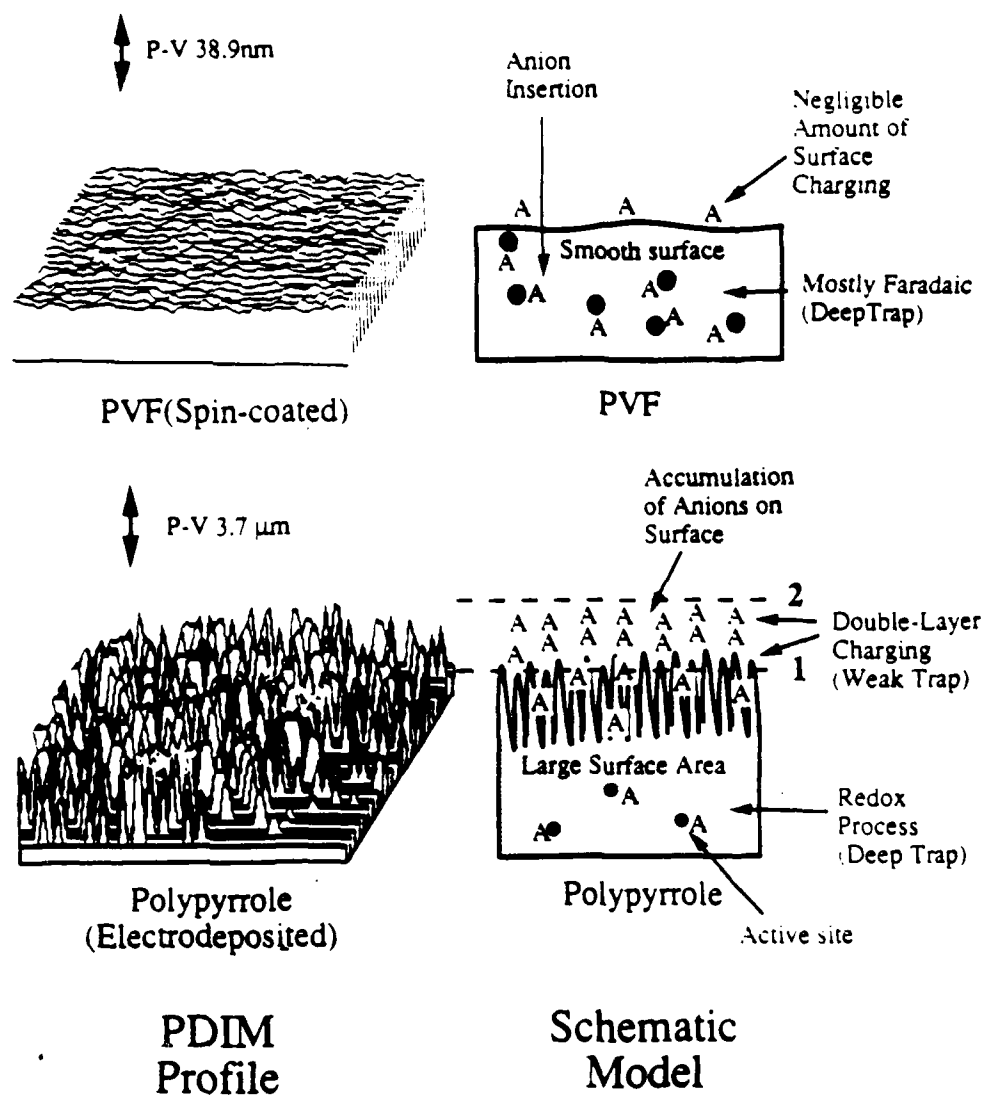


FIGURE 9 Phase detection interferometric microscopic profiles for PPy and PVF films.